Uplift of sedimentary basins in an extensional setting as a result of the migration of a thermal anomaly

Beniest, A.(a,b), Sassi, W.(b), Guichet, X.(b), Matenco, L.(c), Burov, E.(a), Leroy, S.(a), 2016

a) UMR 7193 Institut des Sciences de la Terre de Paris, Université Pierre et Marie Curie, Paris 06, Paris , France: anouk.beniest@etu.upmc.fr; b) IFP Energies nouvelles,Ruei-Malmaison, France; c) Utrecht University, Faculty of Earth Science, Utrecht, The Netherlands

Contact author: anouk.beniest@ifpen.fr

1. Introduction

The formation of sedimentary basins in a purely extensional setting is traditionally related to active tectonic processes during the syn-rift phase and passive processes such as thermal subsidence during the post-rift phase. In a purely extensional setting there is no room for uplift events.

Can unconformities that are observed on seimic data, and are interpreted as such, be explained with the lateral displacement of a mantle anomaly?

2. Model setup

a. Physical fundamentals

- $\rho_{off} g_i + \frac{\partial \sigma_{ij}}{\partial x_j} = \rho_i \frac{\partial V_i}{\partial t}$ Dynamic law (Newton)
- $\frac{\partial h}{\partial t} = k_{erosion} \frac{\partial^2 h}{\partial x^2}$ Erosion sedimentation
- $\frac{D\sigma}{Dt} = F(\sigma, \mathbf{u}, \mathbf{V}, \nabla \mathbf{V}, ..., T, ...)$ Constitutive laws
- $\frac{\partial T}{\partial t} = \frac{\partial}{\partial x_i}\left(X \frac{\partial T}{\partial x_i}\right) + \frac{H_r}{\rho_{off} C_p} - V_i \frac{\partial T}{\partial x_i}$ Heat equation

b. Geometrical setup

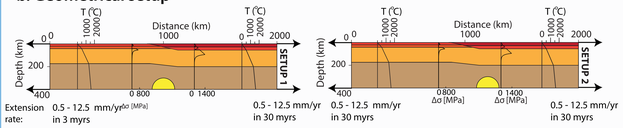

c. Thermal parameters

Thermal property	Value	Unit
Surface temperature	10	°C
Temperature at the bottom of the thermal lithosphere	1330	°C
Thermal conductivity crust	2.5	W/m °C
Thermal conductivity mantle	3.5	W/m °C

Thermal property	Value	Unit
Radiogenic heat production at surface	1.5E-9	W/kg
Radius radiogenic heat	10	km
Thermo-tectonic age of the lithosphere	500	myr
Surface heat flow	40	mW/m^2
Mantle heat flow	15	mW/m^2

d. Rheological strength envelopes

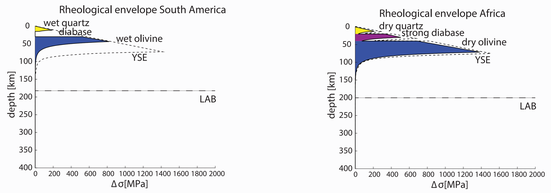

3. Geological setting

a. Regional setting

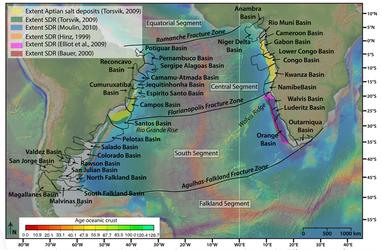

Figure 3.1. Bathymetric map overlain by map with magnetic ages indicating the different times of opening: Rifting in the South Segment started around 132 Ma, rifting in the central segment started around 112 Ma. opened before Central segment). The four segments of the South Atlantic are shown. The investigated transect is the Colorado-Basin Orange Basin. The red line indicates the location of the seismic section below. data from Ryan et al., 2009 and Müller et al., 1997

b. Crustal setting

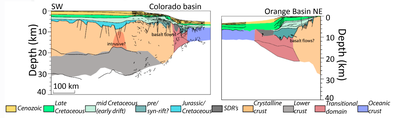

Figure 3.2. Crustal cross-section through the conjugate Colorado Basin and Orange Basin after Blaich, et al., 2013. Note that the package of Late Cretaceous sediments (post-rift) is thicker in the Orange basin then in the Colorado Basin.

c. Basin infill (Orange Basin)

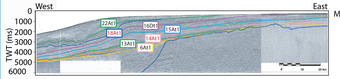

Figure 3.3. Seismic line located perpendicular to the margin of the Orange Basin (see map for exact location). Interpretation shows major and minor unconformities in the post-rift/drift phase. After Paton et al., 2008.

Unconformities observed on seismic data in the Orange Basin:

- 6At1: syn-rift - transition unconformity
- 13At1: transition - drift unconformity
- 13Et1: 1st drift unconformity: coinciding with drop in eustatic sea-level
- 14At1: 2nd drift unconformity: not coinciding with drop in eustatic sea-level
- 15At1: 3rd drift unconformity: coinciding with drop in eustatic sea-level
- 16Dt1: 4th drift unconformity: possibly coinciding with drop in eustatic sea-level
- 17At1: 5th drift unconformity: possibly coinciding with drop in eustatic sea-level
- 18At1: 6th drift unconformity: not coinciding with drop in eustatic sea-level
- 22At1: 7th drift unconformity: coinciding with drop in eustatic sea-level

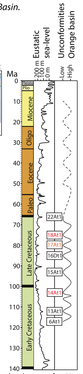

Figure 3.4. a) Eustatic Sea-level curve after Haq et al., 1987; b) Relative base basin 'high' or 'low'.

4. Model results

a. Setup 1

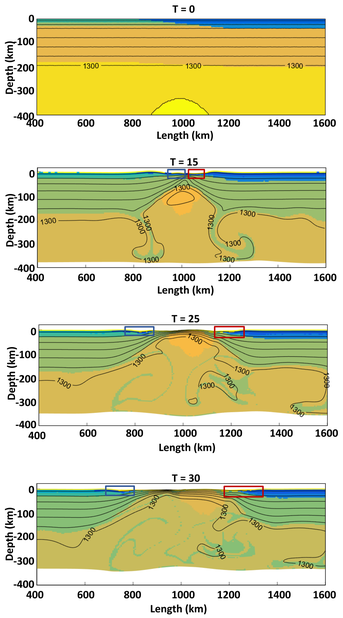

b. Setup 2

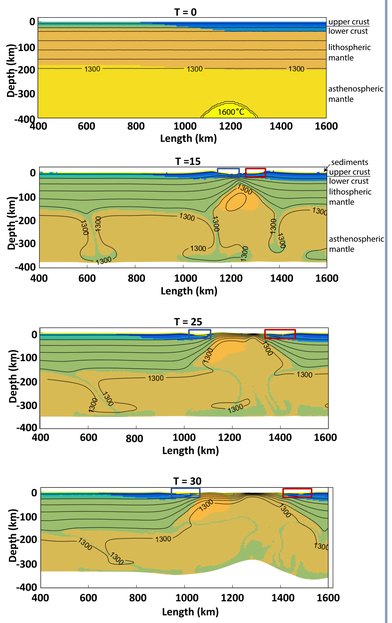

c. Vertical displacement of the basin's base and topography on both sides of the modelled margins

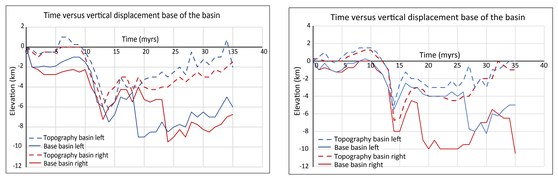

- Vertical displacements of the basin's base is in the order of 100's of meters.
- The topographic evolution of both basins is comparable in terms of depth and geometry allthough the right side is constantly at lower elevation.

5. Discussion

A number of post-rift unconformities on the seismic data cannot be explained with the eustatic sealevel curve of Haq et al., 1987, they have a tectonic origin.

Even though the cell-size of the model influences the modelled basin depth, a component of vertical displacement (up and down) in the post-rift phase is observed.

The topography being constantly lower on the right side of both models might be the result of the initial rheological parameters.

The onset of the thickness variation over time (fig. 5.1) is contemporaneous with break-up. It could be the transition change from symmetric rifting/early drift to a-symmetric spreading.

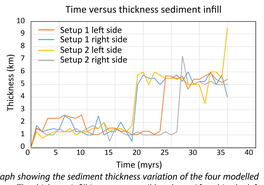

Figure 5.1. Graph showing the sediment thickness variation of the four modelled basins over time. The thickness infill is constant until break-up. After this, the left basin of Setup 1 and the right basin of Setup 2 show a sudden thickness increase.

6. Conclusion

- It is possible to create uplift episodes triggered by a mantle anomaly.
- The order of magnidue of the vertical variations is within 100's of meters, not of kilometers.
- The thickness variation of the basin infill observed in both models might be related to a change from symmetric to a-symmetric spreading.

7. Future work

- A seismic stratigraphic study of a rifted margin basin could provide more inside into the minor unconformities and relative timing of the vertical movements of the basins.
- The thermal and dynamic results from this modelling excercise can be used as input for basin models to investigate the impact of ma processes.

8. References

1. Bauer, K., Neben, S., Schreckenberger, B., Emmerman, R., Hinz, K., Fechner, N., Gohl, K., Schulze, A., Trumbull, R.B., Weber, K., 2000. Deep structure of the Namibia continental margin as derived from integrated geophysical studies. J. Geophys. Res. 105, 25,829–25,853.1.
2. Blaich, O.A., Faleide, J.I., Tsikalas, F., Gordon, A.C., Mohriak, W., 2013. Crustal-scale architecture and segmentation of the South Atlantic volcanic margin. Geol. Soc. London, Spec. Publ. 369, 167–183. doi: 10.1007/s11001-009-9077-x.
3. Elliot et al., G.M., Berndt, C., Parson, L. M., 2009. The SW African volcanic rifted margin and the initiation of the Walvis Ridge, South Atlantic. Marine Geophysical Research, 30, 207-214.
3. Haq, B.U., Hardenbol, J., Vail, P.R., 1987. Chronology of Fluctuating Sea Levels Since the Triassic. Science (80-.). 235, 1156 – 167.
4. Hinz, K., Neben, S., Schreckenberger, B., Roeser, H.A., Block, M., Goncalves de Souza, K., Meyer, H., 1999. The Argentine continental margin north of 48 S: sedimentary successions, volcanic activity during breakup. Mar. Pet. ... 16, 1–25. doi:10.1016/S0264-8172(98)00060-9
5. Moulin, M., Aslanian, D., Unternehr, P., 2010. A new starting point for the South and Equatorial Atlantic Ocean. Earth Sci. Rev. 98, 1–37. doi:10.1016/j.earscirev.2009.08.001
6. Müller, R.D., Roest, W.R., Royer, J.-Y., Gahagan, L.M., Sclater, J.G., 1997. Digital isochrons of the world's ocean floor. J. Geophys. Res. 102, 3211–3214.
8. Paton, D.A., van der Spuy, D., di Primio, R., Horsfield, B., 2008. Tectonically induced adjustment of passive-margin accomodation space; influence on the hydrocarbon potential of the Orange Basin, South Africa. AAPG Bulletin, v. 92, 5, 589 - 609
9. Ryan, W.B.F., Carbotte S.M., Coplan, J.O., O'Hara, S., Melkonian, A., Arko, R., Weissel, R.A., Ferrini, V., Goodwillie, A., Nitsche, F., Bonczkowski, J., Zemski, R., 2009. Global Multi-Resolution Topography synthesis. Geochemistry, Geophys. Geosystems , doi:10. doi:10.1029/2008GC002332
10. Torsvik, T.H., Rousse, S., Labails, C., Smethurst, M.A., 2009. A new scheme for the opening of the South Atlantic Ocean and the dissection of an Aptian salt basin. Geophys. J. Int. 177, 1315–1333. doi:10.1111/j.1365-246X.2009.04137.x